27710

National Library of Canada | Bibliothèque nationale du Canada

CANADIAN THESES ON MICROFICHE | THÈSES CANADIENNES SUR MICROFICHE

NAME OF AUTHOR/*NOM DE L'AUTEUR* EMMANUEL N. MOFOR

TITLE OF THESIS/*TITRE DE LA THÈSE* MOTION OF THRESHED GRAINS ON AN OSCILLATING PAN.

UNIVERSITY/*UNIVERSITÉ* UNIVERSITY OF ALBERTA, EDMONTON

DEGREE FOR WHICH THESIS WAS PRESENTED/*GRADE POUR LEQUEL CETTE THÈSE FUT PRÉSENTÉE* M. SC.

YEAR THIS DEGREE CONFERRED/*ANNÉE D'OBTENTION DE CE GRADE* 1976

NAME OF SUPERVISOR/*NOM DU DIRECTEUR DE THÈSE* DR. H. P. HARRISON.

Permission is hereby granted to the NATIONAL LIBRARY OF CANADA to microfilm this thesis and to lend or sell copies of the film.

The author reserves other publication rights, and neither the thesis nor extensive extracts from it may be printed or otherwise reproduced without the author's written permission.

L'autorisation est, par la présente, accordée à la BIBLIOTHÈQUE NATIONALE DU CANADA de microfilmer cette thèse et de prêter ou de vendre des exemplaires du film.

L'auteur se réserve les autres droits de publication; ni la thèse ni de longs extraits de celle-ci ne doivent être imprimés ou autrement reproduits sans l'autorisation écrite de l'auteur.

DATED/*DATÉ* 17th DEC '75 SIGNED/*SIGNÉ* [signature]

PERMANENT ADDRESS/*RÉSIDENCE FIXÉ* c/o PAUL MBANGWANA,
UNIVERSITY OF CAMEROON,
CAMEROON, WEST AFRICA.

NL-91 (3-74)

INFORMATION TO USERS

THIS DISSERTATION HAS BEEN
MICROFILMED EXACTLY AS RECEIVED

This copy was produced from a microfiche copy of the original document. The quality of the copy is heavily dependent upon the quality of the original thesis submitted for microfilming. Every effort has been made to ensure the highest quality of reproduction possible.

PLEASE NOTE: Some pages may have indistinct print. Filmed as received.

Canadian Theses Division
Cataloguing Branch
National Library of Canada
Ottawa, Canada K1A 0N4

AVIS AUX USAGERS

LA THESE A ETE MICROFILMEE
TELLE QUE NOUS L'AVONS RECUE

Cette copie a été faite à partir d'une microfiche du document original. La qualité de la copie dépend grandement de la qualité de la thèse soumise pour le microfimage. Nous avons tout fait pour assurer une qualité supérieure de reproduction.

NOTA BENE: La qualité d'impression de certaines pages peut laisser à désirer. Microfilmée telle que nous l'avons reçue.

Division des thèses canadiennes
Direction du catalogage
Bibliothèque nationale du Canada
Ottawa, Canada K1A 0N4

THE UNIVERSITY OF ALBERTA

MOTION OF THRESHED GRAINS ON AN OSCILLATING PAN

by

© EMMANUEL NCHUMULUH MOFOR

A THESIS

SUBMITTED TO THE FACULTY OF GRADUATE STUDIES AND RESEARCH

IN PARTIAL FULFILMENT OF THE REQUIREMENTS FOR THE DEGREE

OF MASTER OF SCIENCE

IN

AGRICULTURAL ENGINEERING

DEPARTMENT OF AGRICULTURAL ENGINEERING

EDMONTON, ALBERTA

SPRING, 1976

THE UNIVERSITY OF ALBERTA

FACULTY OF GRADUATE STUDIES AND RESEARCH

The undersigned certify that they have read, and recommend to the Faculty of Graduate Studies and Research for acceptance, a thesis entitled "Motion of Threshed Grains on an Oscillating Pan," submitted by Emmanuel Nchumuluh Mofor in partial fulfilment of the requirements for the degree of Master of Science.

.....
Supervisor

.....

.....

.....

Date Dec 11 1975

ABSTRACT

The motion of a prolate spheroid shaped grain on an oscillating pan, as affected by pan frequency, slope, crank radius and coefficient of friction between pan and grain (kernel), was studied. Oscillating pans are used extensively as conveyors and screens in seed handling and cleaning. To know the relationship between the variables noted above would be useful because they affect the velocity of the kernels on the pan surface. The kernel velocity and therefore the feed rate affects the efficiency of the separation process.

The motion of a wheat kernel was observed on an oscillating pan at various combinations of pan frequency, slope and crank radius. An additional mode of motion was observed and was tentatively defined as a spinning and sliding mode. Because two modes of motion of the prolate spheroid are related to the natural rocking frequency of the spheroid and the pan frequency, an expression was derived to calculate the natural rocking frequency of a prolate spheroid. Equations of motion were derived for three modes of motion and experimental kernel velocities determined for the rocking and sliding mode. The velocities obtained were observed to increase with an increase in pan frequency, slope and crank radius as predicted by the derived equations.

TABLE OF CONTENTS

CHAPTER		PAGE
I	LITERATURE REVIEW AND OBJECTIVES	1
	1.1 Introduction	1
	1.2 Literature Review	2
	1.2.1 Riding Motion - Category A	2
	1.2.2 Riding and Sliding - Cagegory A	3
	1.2.3 Sliding - Category A	3
	1.2.4 Hopping - Category A and B	4
	1.2.5 Rolling and Sliding - Category B . . .	5
	1.2.6 Rocking and Sliding - Category B . . .	6
	1.2.7 Summary	7
	1.3 Objectives	7
	1.4 Study Method	8
II	FACILITIES AND ROCKING FREQUENCIES	9
	2.1 Description of Facilities	9
	2.2 Experimental Natural Rocking Frequencies	10
	2.3.1 Observation of the Motion of a Prolate Spheroid on an Oscillating Pan	11
	2.3.2 Rolling and Sliding Mode	13
	2.3.3 Rocking and Sliding Mode	15
	2.3.4 Spinning and Sliding Mode	17
	2.4.1 Theoretical Natural Rocking Frequency .	18
	2.4.2 Derivation of Natural Rocking Frequency Equation	18

CHAPTER PAGE

2.4.3 Results, Discussion and Conclusions . . 26

III EQUATIONS OF KERNEL MOTION 29

3.1 Introduction 29

3.2 Assumptions 29

3.3 Motion of Oscillating Pan 32

3.4.1 Rolling and Sliding Mode 34

3.4.2 Rolling With Sliding Phase 36

3.4.3 Rolling Without Sliding Phase 39

3.5 Rocking and Sliding Mode 41

3.6 Spinning and Sliding Mode 43

3.7 Hopping Mode 43

IV RESULTS, DISCUSSION, SUMMARY AND CONCLUSIONS . 45

4.1 Experimental Kernel Velocities 45

4.2 Discussion of Results 47

4.3 Summary and Conclusions 49

BIBLIOGRAPHY 51

APPENDICES 54

LIST OF TABLES

TABLE	DESCRIPTION	PAGE
2.1	Experimental Natural Rocking Frequencies . . .	11
2.2	Natural Rocking Frequencies of Two Prolate Spheroids	25
3.1	Regimes of Kernel Motion	35
4.1	Experimental Wheat Kernel Velocities	46

LIST OF FIGURES

FIGURE		PAGE
2.1	Schematic of Oscillating Pan	9
2.2	Rolling and Sliding Mode	13
2.3	Pan Displacement Against Crank Angle	14
2.4	Rocking and Sliding Motion	15
2.5	Rocking Orientations of Prolate Spheroid . . .	16
2.6	Rolling and Sliding mode	17
2.7	Rocking and Sliding mode	17
2.8	Spinning and Sliding mode	17
2.9	Hopping mode	17
2.10	Rocking Prolate Spheroid	20
2.11	Schematic of Prolate Spheroid	26
2.12(a)	Steel Prolate Spheroid - Rolling Motion . . .	27
2.12(b)	Wheat Kernel - Rolling Motion	27
2.13(a)	Steel Prolate Spheroid - Rocking Motion . . .	27
2.13(b)	Wheat Kernel - Rocking Motion	27
3.1	Hopping With Sliding	31
3.2	Hopping Without Sliding	31
3.3	Velocities and Accelerations of Pan and Kernel	35
3.4	Free-body Diagram of Kernel in the Normal Roll Down Mode With Sliding	36
3.5	Rolling With and Without Sliding Motion . . .	40
3.6	Free-body Diagram of Kernel Sliding Down the Pan Surface	41

FIGURE		PAGE
4.1	Kernel Path on Pan Surface	45
4.2	Aperture Orientation for Rolling and Sliding Seeds	47
4.3	Aperture Orientation for Rocking and Sliding Seeds	47

CHAPTER I

LITERATURE REVIEW AND OBJECTIVES

1.1 Introduction

Oscillating pans are used to convey granular materials by achieving a relative motion between the material and the pan. The pan oscillates without a net translation of its own but imparts a relative motion to the material on its surface. The material travels with a cyclic variation in velocity along the pan surface.

Oscillating pans offer many advantages[4] over augers because they are self cleaning; there is a minimum degradation of material and their power requirements are low. According to Berry[1] they can be constructed cheaply, being of simple design and not requiring any expensive materials. The drive however is complicated by the need to use a slider-crank mechanism. They are able to convey dirty, abrasive granular materials without damage, and do not become choked, compared to augers.

The primary use of oscillating pans in agriculture and related industries is in seed cleaning, grading of seed, grains and fruit. Clean and graded seeds and grains are used for milling, seeding, brewing and commercial trading.

In seed cleaning and grading of grains, the kernels are fed onto a perforated oscillating pan. Undersized kernels,

foreign material and dirt pass through the perforations or apertures. The clean and oversized kernels go over the end of the screen and are collected in a hopper. To remove oversized debris, a pre-screen is used. The undersized objects for this additional screen are all the kernels, foreign material and dirt.

1.2 Literature Review

The motion of grains on an oscillating pan can be broadly divided into two categories, depending on the shape of the grain. For one category (A), the grain is of irregular shape, such as a corn or maize kernel. For the other category (B), the shape of the grain is an approximate prolate spheroid, such as a wheat kernel. The literature review has been organized on the basis of these categories.

1.2.1 Riding Motion - Category A

Berry[1,2] defines riding of an object on an oscillating pan as the motion of an object in which there is no relative motion between the object and the pan; hence the object moves with the pan surface throughout a crank cycle. He derived dimensionless ratios or terms using the variables of kinetic and static coefficients of friction, conveyor frequency and amplitude, and acceleration due to gravity. The relationship between the dimensionless ratios states the condition under which riding would or would not occur.

1.2.2 Riding and Sliding - Category A

Berry[1,2] states that riding and sliding of an object occurs if the object rides for part of the crank cycle and slides, or has motion relative to the pan, for the remainder. The relationship between the dimensionless terms derived by Berry[1,2] can be used to calculate the conveyor frequency range within which riding and sliding of an object would occur.

1.2.3 Sliding - Category A

Berry[1,2] identifies sliding of an object as motion in which there is continuous contact and relative motion between the object and the pan surface. The object moves either positively or negatively (i.e. down or up the pan surface) but it slides throughout a crank cycle. The conveyor frequency range within which this motion would occur can be calculated from the dimensionless terms derived by Berry.[1,2] He has also derived and solved graphically a non-linear differential equation of this motion for the acceleration of an object on an oscillating conveyor. The equation is derived in terms of conveyor frequency, kinetic coefficient of friction between object and conveyor surface, acceleration due to gravity and angle of attack. The last variable is the inclination of the support arms of the oscillating conveyor with respect to the vertical. Shertz and Hazen[14] have also derived differential equations for positive and negative accelerations of a sliding object on an oscillating conveyor in terms of conveyor

frequency, amplitude, slope, kinetic coefficient of friction and gravity. The conveyor used in the study by Schertz and Hazen had a slope rather than an angle of attack and hence their equation is different from that derived by Berry. Garvie[6] has derived acceleration equations for positive and negative sliding of grain on an oscillating sieve in terms of sieve frequency, amplitude, slope, acceleration due to gravity, kinetic coefficient of friction and the time periods associated with the beginning of sliding down or up the sieve. He has also developed an equation that could be used to calculate a suitable grain velocity range for efficient screening.

1.2.4 Hopping - Category A and B

Berry[2] states that hopping of an object occurs when the object looses contact with the pan surface. This happens when the vertical acceleration of the pan downward is greater than that due to gravity. He has developed an equation for the conveyor frequency range in terms of acceleration due to gravity, static coefficient of friction and conveyor displacement, within which the object would loose contact with the conveyor. Schertz and Hazen[14] have stated the condition for a free fall of an object as a function of gravitational acceleration and the vertical acceleration of the conveyor. Harrison[10] has derived differential equations of motion for kernels in an air stream rebounding from a non-oscillating

surface. Using an analog computer, these equations were used to simulate a kernel rebound trajectories in a combine shoe. In later work, Harrison[11] used the equations to simulate the motion of threshed particles that are subjected to the rotary motion of walkers in a combine harvester. He notes that the transition from the rotary to free-fall regime occurs when the vertical acceleration of the walker downwards is equal to the acceleration of gravity. Bottcher[3] notes the same for an oscillating conveyor. He states that in a crank period t, an object leaves the conveyor surface at the moment t_s and contacts the surface again at the moment t_a. Mathematical expressions for these moments of detachment and impact, t_s and t_a, were derived by him in terms of conveyor frequency, amplitude and angle of attack. An expression for the maximum height of the hop or jump of the object from the conveyor surface was also derived in terms of the above variables. He has also expressed the mean velocity of the object in the horizontal direction in terms of moments of detachment and impact t_s and t_a, acceleration due to gravity, conveyor frequency and angle of attack.

1.2.5 Rolling and Sliding - Category B

Hann and Gentry[8] observed that an ellipsoidal object rolls and slides on an oscillating conveyor surface when the conveyor is operated at frequencies below the natural rocking frequency of the object. Though Hann and Gentry identify the

object as an ellipsoid, it likely was a prolate spheroid. They state that in the rolling and sliding mode, the orientation of the prolate spheroid is with the major axis perpendicular to the direction of conveyor motion. They developed equations for a prolate spheroid which exhibits rolling resistance due to surface deformation but simulated the motion of a rubber ball. It is not clear why a rubber ball was used instead of a prolate spheroid.

1.2.6 Rocking and Sliding - Category B

Hann and Gentry[8] observed rocking and sliding and they state that a prolate spheroid rocks and slides on an oscillating conveyor when the conveyor is operated at frequencies above the natural rocking frequency of the spheroid. The orientation of the spheroid is with the major axis parallel to the direction of conveyor motion. They did not derive equations for this mode of motion and hence it was not simulated. The work of Henderson and Newman[12] is useful in studying category B motion because they investigated a prolate object which has a similar shape to a prolate spheroid. They observed that the orientation of a prolate object on a horizontal plane was related to the natural frequency of rocking of the prolate object and the frequency of oscillation of the surface. They provided physical and analytical explanations of the phenomenon together with related experimental results. The oscillating prolate object is described mathematically as a forced vibration of a viscously damped single degree of freedom system. The

forcing frequency is provided by the oscillation of the horizontal surface. They derived a forced vibration equation for the oscillating prolate object by using Lagrange's equation. The equation is useful in describing the prolate object orientations on the horizontal surface as a function of the frequency of oscillation of the prolate object and the surface.

1.2.7 Summary

As can be noted from the above, not much work has been done on the motion of threshed grains on an oscillating pan, particularly the motion of grains in category B. Because of the importance of grain cleaning and grading in the agricultural industry, research on motion of kernels on an oscillating pan was undertaken.

1.3 Objectives

The study was limited to motion of prolate spheroid shaped grains on an oscillating pan; that is category B. The objectives of the study were:

(a) to determine the relationship between the orientation of a prolate spheroid on an oscillating pan and the natural rocking frequency of the spheroid as affected by the pan frequency, and hence develop an equation for the natural rocking frequency of a prolate spheroid.

(b) to derive equations of motion of prolate spheroid shaped kernels on an oscillating pan.

1.4 Study Method

In part 1, the motion of a wheat kernel was observed on an oscillating pan using various combinations of pan frequency, amplitude and slope. Since a wheat kernel has a shape similar to a prolate spheroid, large sizes of prolate spheroids were made of steel and aluminium to facilitate the study. The natural rocking frequencies of these spheroids were determined experimentally and their motions observed on the oscillating pan at various pan frequencies, amplitudes and slopes. An expression was derived to determine the natural rocking frequencies of prolate spheroids. The expression was used to calculate the natural rocking frequencies of the steel and aluminium spheroids. The theoretical and experimental natural rocking frequencies were compared.

In part 2, differential equations of motion are derived for various modes of motion observed. For the rocking and sliding mode the velocity of a wheat kernel on an oscillating pan was determined experimentally. The relationship between the velocity and some independent variables were discussed.

CHAPTER II

FACILITIES AND ROCKING FREQUENCIES

2.1 Description of Facilities

A schematic of the oscillating pan used in the study of prolate spheroid motion is shown in figure 2.1 (a and b).

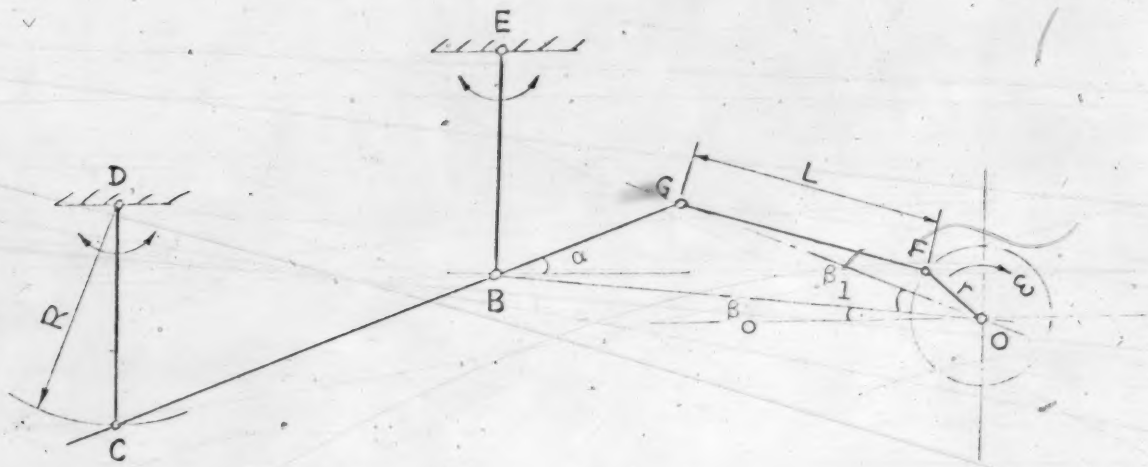

(a)

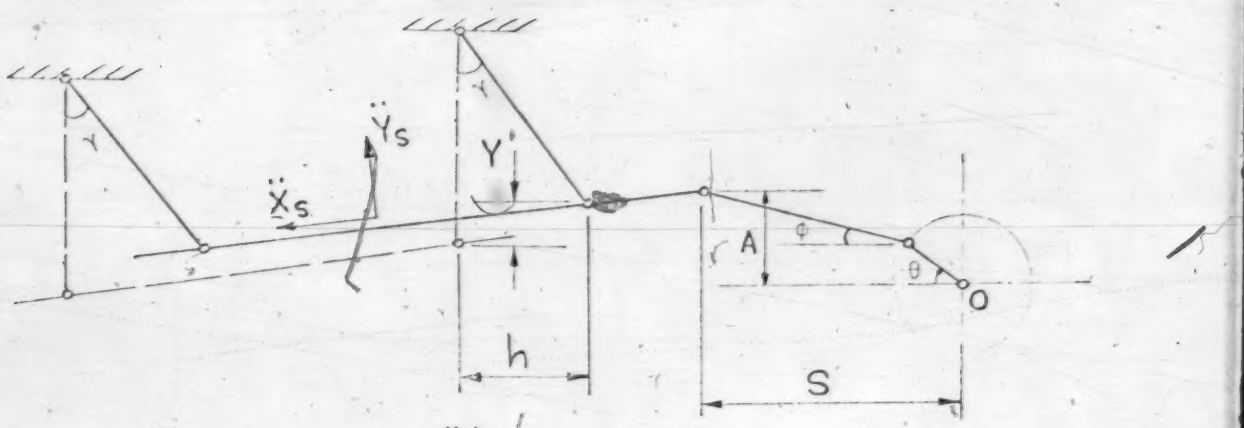

(b)

Figure 2.1 (a and b) Schematic of oscillating pan

The pan BC and the rod AB were rigidly connected and thus AC moved as one piece in a non-linear translation. The pan was 31 in. long by 13 in. wide. The grain was fed onto the pan at B and was observed as it moved along the pan to C. The grain was collected in a hopper after passing C. The suspension arms DC and EB were 12 in. long and D was adjustable relative to E to achieve various pan slopes or angles (α). The angle β_o was 12.8°. The pitman arm AF was 4.5 in. long and the crank radius r could be varied from zero to 0.75 in. Various pan frequencies were obtained by using different sizes of pulleys mounted on the pan drive shaft at 0. The pulleys were driven by a constant speed electric motor through a "V" belt. A $\frac{1}{4}$ in. square grid, 1 ft. and 1 in. long and 1 ft. wide was mounted 3 in. above the pan surface; the mounting being done on the pan frame. The use of the grid was to aid in observing the orientation of prolate spheroids on the oscillating pan surface. A 16 mm. movie camera with provision for slow motion photography was used as an additional aid in observing the motion of objects on the pan.

2.2 Experimental Natural Rocking Frequencies

Two large prolate spheroids were made of steel and aluminium because it is easier to determine their natural rocking frequencies than it is for kernels of small grains.

Each prolate was disturbed by displacing the centre of mass in the vertical plane to start it rocking and the number of oscillations per minute were calculated. The results of three trials are shown in Table 2.1.

TABLE 2.1

EXPERIMENTAL NATURAL ROCKING FREQUENCIES

Prolate Spheroid	a (in.)	b (in.)	No. of Trials 1 (CPM)	2 (CPM)	3 (CPM)	Average (CPM)
Steel	2.00	1.00	147	152	151	150
Aluminium	1.25	0.50	180	192	186	186

2.3.1 Observation of the Motion of a Prolate Spheroid on an Oscillating Pan

The motions of the prolate spheroids in Table 2.1 were observed on the oscillating pan (see figure 2.1) at various pan frequencies, amplitudes and slopes. As already noted by Hann and Gentry,[8] it was observed that at a pan frequency (150 CPM) below the natural rocking frequency of the aluminium spheroid (186 CPM), the orientation of the spheroid was with the major axis perpendicular to the direction of pan motion and at pan frequencies (303 and 405 CPM) above the natural rocking frequency of the spheroid, the orientation

of the spheroid was with the major axis parallel to the direction of pan motion. With the major axis perpendicular to the direction of pan motion (pan frequency less than the natural rocking frequency), it was observed that the spheroid rolls and slides on the pan surface. In the rolling and sliding mode, there was rolling with and without sliding (phases) in a single crank cycle. With the major axis of the spheroid parallel to the direction of pan motion (pan frequency greater than the natural rocking frequency), it was observed that the spheroid rocks and slides on the pan surface. In the rocking and sliding mode, there was rocking without sliding (i.e. rocking and riding) and rocking with sliding (phases) in a single crank cycle.

At pan frequencies much above the natural rocking frequency of the spheroid (greater than 405 CPM), the spheroid spun and slid on the pan surface. This motion has not been noted in the literature and therefore this mode is defined as spinning and sliding.

At greater pan frequencies and slopes, it was observed that the spheroid partially lost contact with the pan in a crank cycle; hence hopping on the pan surface. The hopping mode is dependent on both pan frequency and slope.

The modes noted above are the only four motions of a prolate spheroid observed on the oscillating pan. They are described in detail below.

2.3.2 Rolling and Sliding Mode

Figure 2.2 shows a prolate spheroid in the rolling

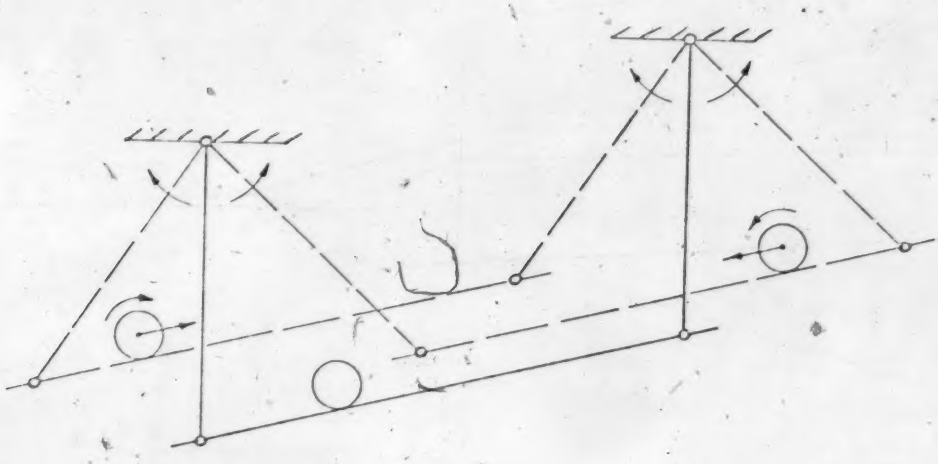

Figure 2.2 Rolling and Sliding Mode

and sliding mode. For this mode the spheroid orientation is with the major axis perpendicular to the direction of pan motion (see Figure 2.6). A more detailed presentation of the motion in this mode is shown in Figure 2.3 where the pan position is shown for various crank angles. The directions of rotation and acceleration of the prolate spheroid at various crank angles during a cycle of pan oscillation are indicated.

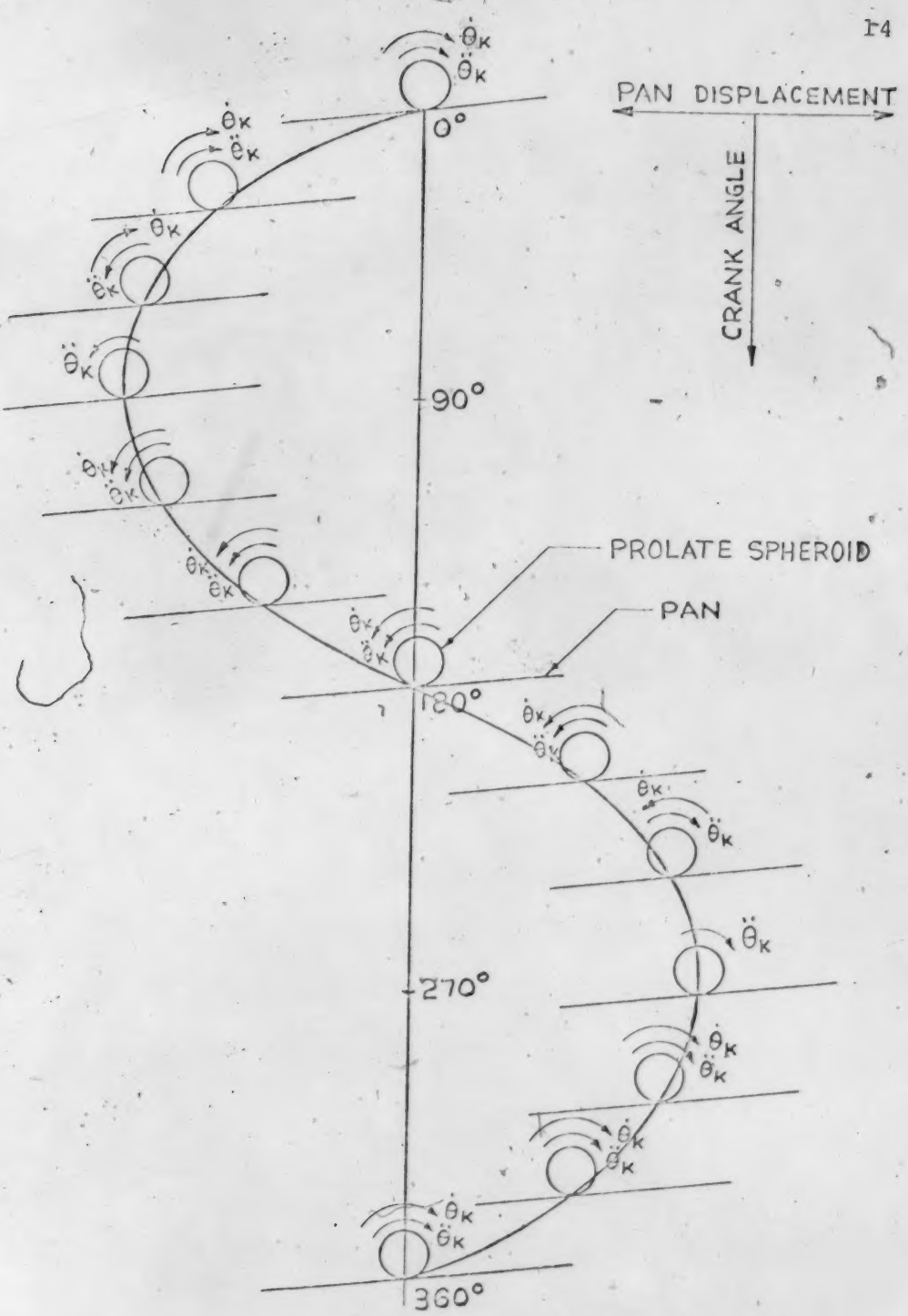

Figure 2.3 Pan displacement against crank angle

2.3.3 Rocking and Sliding Mode

As already noted, rocking and sliding of a spheroid occurs at pan frequencies above the natural rocking frequency of the prolate spheroid.

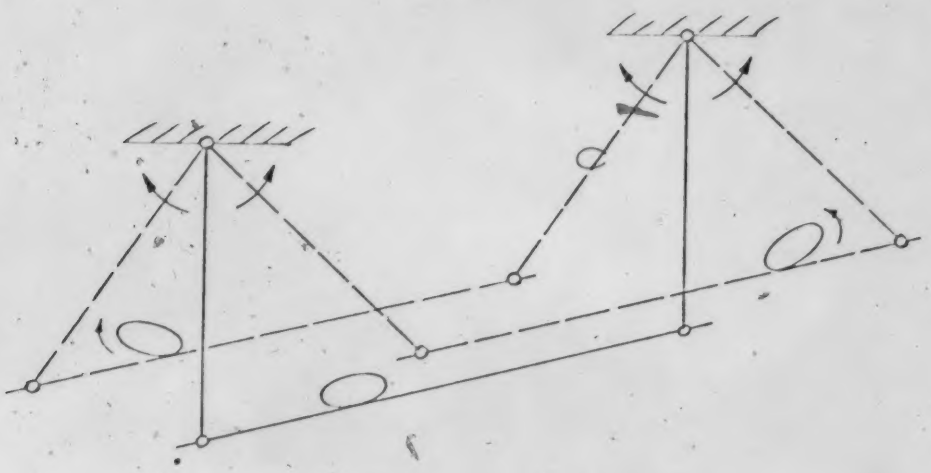

Figure 2.4 Rocking and Sliding Motion

Figure 2.4 shows a prolate spheroid in the rocking and sliding mode. For this mode, the spheroid orientation is with the major axis parallel to the direction of pan motion (see Figure 2.7). At pan frequencies equal to the natural rocking frequency of the spheroid, the spheroid orientation is unstable in the sense that the mode of conveyance is a mixture of rolling and sliding with rocking and sliding. Figure 2.5 shows the rotating directions of the spheroid at various crank angles over a cycle of pan oscillation for the rocking and sliding mode.

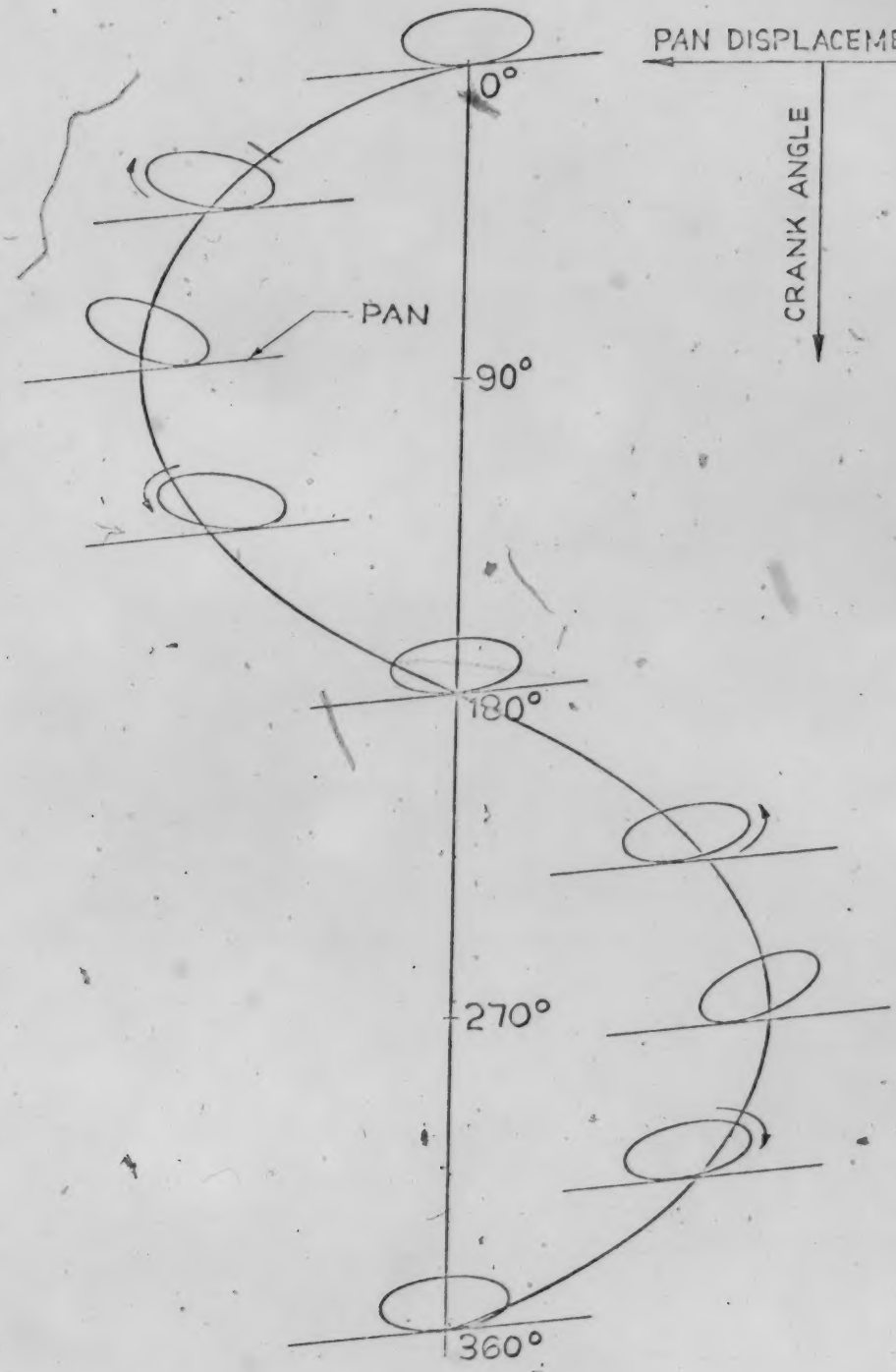

Figure 2.5 Rocking orientations of prolate spheroid

2.3.4 Spinning and Sliding Mode

The third mode of spheroid motion observed was spinning and sliding (see Figure 2.8). As already noted, this mode occurred at pan frequencies much greater than the natural rocking frequency of the spheroid. In this mode, the spheroid spins and slides on the pan surface.

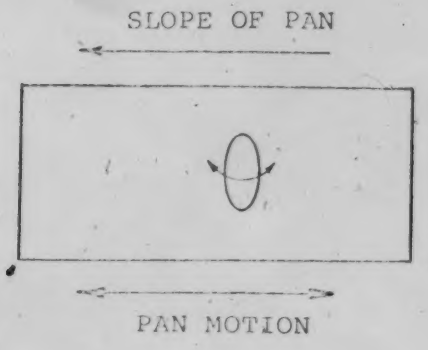

Figure 2.6 Rolling and sliding mode.

Figure 2.7 Rocking and sliding mode.

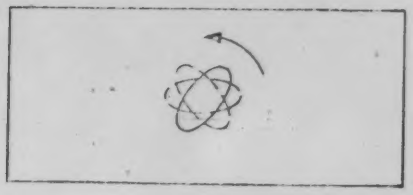

Figure 2.8 Spinning and sliding mode.

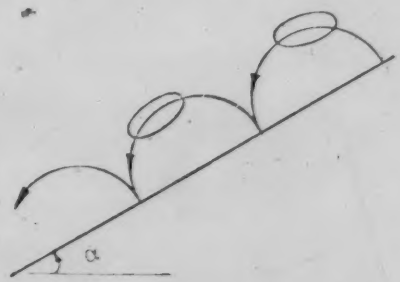

Figure 2.9 Hopping mode.

The fourth and last mode of motion (hopping) occurred at very high pan frequencies and large slopes (see Figure 2.9). The hopping mode is observed to be influenced jointly by the pan frequency and slope. As will be shown later, if the spheroid slides while in contact with the pan surface,

the spheroid trajectory is slightly different from that shown in Figure 2.9.

2.4.1 Theoretical Natural Rocking Frequency

The natural rocking frequency of a prolate spheroid is defined as the number of cycles per unit time the spheroid oscillates when the centre of mass in the vertical plane containing the major axis is displaced. As already noted, the natural rocking frequency of a prolate spheroid determines the mode of conveyance of the spheroid on an oscillating pan. For very small objects which are of prolate spheroid shape, such as wheat kernels, it may not be possible or practical to determine the natural rocking frequency experimentally because the kernels are too small and the oscillations too high to be counted visually. Hence an attempt was made to determine the natural rocking frequency theoretically. This was accomplished by deriving an equation based on the conservation of energy.

2.4.2 Derivation of Natural Rocking Frequency Equation

In determining the natural frequency of free oscillation, the maximum kinetic energy of the spheroid is equated to the maximum potential energy.[19] The equality assumes that the system is conservative, that is, the total energy of the system is constant and is the sum of the potential energy and kinetic energy. The potential energy is

the gravitational potential energy since elastic deformation is neglected; the prolate spheroid being treated as a rigid body. Since the total energy is constant;

$$T + U = \text{constant}^{19} \qquad 2.2.1$$

and $$(d/dt)(T + U) = 0 \qquad 2.2.2$$

where T is the kinetic energy,

U is the potential energy.

As can be seen from equation 2.2.1 if the potential energy is zero, then the kinetic energy is maximum and if the kinetic energy is zero, then the potential energy is maximum. Assuming conservation of energy then;

$$T_{max.} = U_{max.} \qquad 2.2.3$$

The natural rocking frequency of the spheroid can be determined from equation 2.2.3 if the oscillatory motion is harmonic. If the angle of oscillation, β, is small (see Figure 2.10) so that terms higher than β^2 can be neglected, then equation 2.2 is satisfied by:

$$\beta = \beta_o \sin \omega t,$$

which is simple harmonic motion. The vertical displacement of the mass centre, when the spheroid rocks or rotates through the angle β is determined by considering the following.

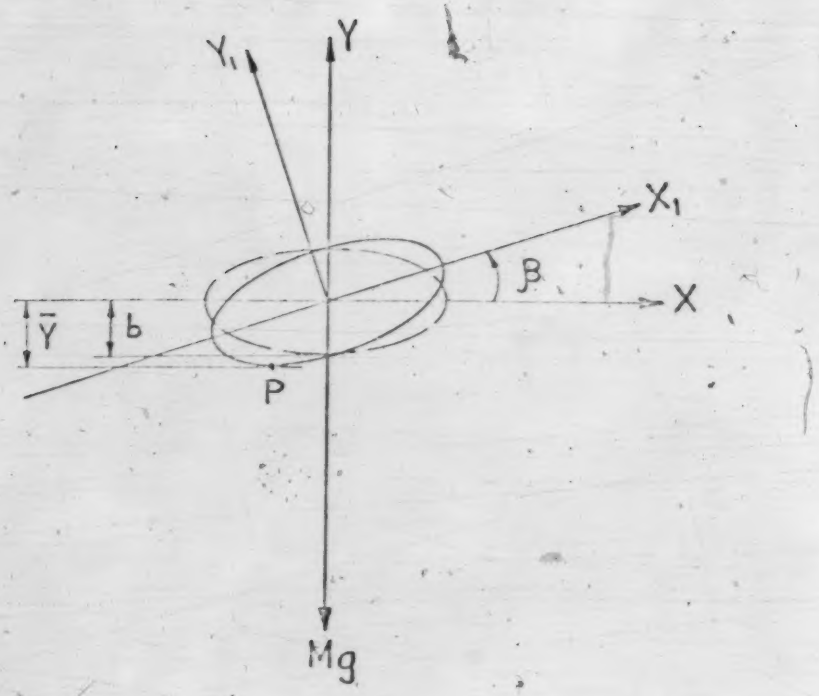

Figure 2.10 Rocking Prolate Spheroid

The equation of the ellipse of revolution with respect to the XY axes is;

$$\frac{X^2}{a^2} + \frac{Y^2}{b^2} = 1, \qquad 2.5.1$$

and the equation of the rotated ellipse with respect to the X_1Y_1 axes is;

$$\frac{X_1^2}{a^2} + \frac{Y_1^2}{b^2} = 1. \qquad 2.5.2$$

The equations for transformation of coordinates are;

$$X_1 = X\cos\beta + Y\sin\beta, \qquad 2.5.3$$

$$Y_1 = -X\sin\beta + Y\cos\beta. \qquad 2.5.4$$

Substituting equations 2.5.3 and 2.5.4 in 2.5.2 gives,

$$\frac{(X\cos\beta+Y\sin\beta)^2}{a^2} + \frac{(-X\sin\beta+Y\cos\beta)^2}{b^2} = 1$$

i.e. $$X^2[\frac{\cos^2\beta}{a^2} + \frac{\sin^2\beta}{b^2}] + 2XY\sin\beta\cos\beta[\frac{1}{a^2} - \frac{1}{b^2}]$$

$$+ Y^2[\frac{\sin^2\beta}{a^2} + \frac{\cos^2\beta}{b^2}] = 1 \qquad 2.5.5$$

which can be put in the form;

$$AX^2 + BXY + CY^2 = 1 \qquad 2.5.6$$

where, $$A = [\frac{\cos^2\beta}{a^2} + \frac{\sin^2\beta}{b^2}] \qquad 2.5.7$$

$$B = 2\sin\beta\cos\beta[\frac{1}{a^2} - \frac{1}{b^2}] \qquad 2.5.8$$

$$C = [\frac{\sin^2\beta}{a^2} + \frac{\cos^2\beta}{b^2}] \qquad 2.5.9$$

Differentiating 2.5.6 with respect to X gives;

$$2AX + BY + BX\frac{dy}{dx} + 2CY\frac{dy}{dx} = 0 \qquad 2.5.10$$

The tangent at point P in figure 2.10 is given by $\frac{dy}{dx} = 0$

Hence equation 2.5.10 reduces to;

$$2AX + BY = 0$$

so that,

$$(Y)_{Y'=0} = -\frac{2AX}{B}$$

$$= \bar{Y} \text{ (see Figure 2.10)} \qquad 2.5.11$$

where $Y' = dy/dx$.

Solving equation 2.5.6 for X,

$$X = -\frac{BY}{2A} \pm \frac{1}{2A}\sqrt{(BY)^2 - 4A(CY^2-1)}$$

and substituting for X from equation 2.5.11;

$$\bar{Y} = \bar{Y} \mp \frac{1}{B}\sqrt{(B\bar{Y})^2 - 4A(C\bar{Y}^2-1)}$$

Hence, $(B\bar{Y})^2 - 4A(C\bar{Y}^2-1) = 0$

and therefore, $\bar{Y} = \sqrt{\frac{A}{AC-B^2/4.}}$ 2.5.12

From equations 2.5.7 and 2.5.9;

$$AC = [\frac{\cos^2\beta}{a^2} + \frac{\sin^2\beta}{b^2}]\ [\frac{\sin^2\beta}{a^2} + \frac{\cos^2\beta}{b^2}]$$

$$= \frac{1}{a^4}\cos^2\beta\sin^2\beta + \frac{1}{a^2b^2}\cos^4\beta + \frac{\sin^4\beta}{a^2b^2} + \frac{\sin^2\beta\cos^2\beta}{b^4}$$

$$= \sin^2\beta\cos^2\beta[\frac{1}{a^4} + \frac{1}{b^4}] + \frac{1}{a^2b^2}(\cos^4\beta+\sin^4\beta)$$

$$= \sin^2\beta\cos^2\beta[\frac{1}{a^4} + \frac{1}{b^4}] + \frac{1}{a^2b^2}[(\cos^2\beta+\sin^2\beta)^2-2\cos^2\beta\sin^2\beta]$$

$$= \sin^2\beta\cos^2\beta[\frac{1}{a^4} + \frac{1}{b^4}] + \frac{1}{a^2b^2}[1-2\cos^2\beta\sin^2\beta]$$

$$= \sin^2\beta\cos^2\beta[\frac{1}{a^4} + \frac{1}{b^4}] - \frac{2}{a^2b^2}\cos^2\beta\sin^2\beta + \frac{1}{a^2b^2}$$

From equation 2.5.8;

$$B^2 = \{2\sin\beta\cos\beta[\frac{1}{a^2} - \frac{1}{b^2}]\}^2$$

$$= 4\sin^2\beta\cos^2\beta\left[\frac{1}{a^4} + \frac{1}{b^4}\right] - \frac{8}{a^2b^2}\sin^2\beta\cos^2\beta.$$

Consequently,

$$\frac{B^2}{4} = \sin^2\beta\cos^2\beta\left[\frac{1}{a^4} + \frac{1}{b^4}\right] - \frac{2}{a^2b^2}\sin^2\beta\cos^2\beta$$

and, $AC - B^2/4 = \frac{1}{a^2b^2}$

Hence equation 2.5.12 becomes;

$$\bar{Y} = \sqrt{\frac{A}{1/a^2b^2}}$$

$$= ab\sqrt{A} \qquad 2.5.13$$

Equation 2.5.7 gives;

$$A = \left[\frac{\cos^2\beta}{a^2} + \frac{\sin^2\beta}{b^2}\right]$$

$$= \frac{\cos^2\beta}{a^2}\left[1 + \frac{a^2}{b^2}\tan^2\beta\right]$$

and, $\sqrt{A} = \frac{\cos\beta}{a}\left[1 + \frac{a^2}{b^2}\tan^2\beta\right]^{1/2}$

Consequently, $\bar{Y} = b\cos\beta\left[1 + \frac{a^2}{b^2}\tan^2\beta\right]^{1/2}$

The following Taylor series expansions are used;

$$\cos\beta = 1 - \frac{\beta^2}{2} + 0(\beta^3),$$

$$\tan^2\beta = \beta^2 + 0(\beta^3)$$

Hence, $\bar{Y} = b\{1 + (\frac{a^2}{b^2} - 1/2)\beta^2\} + 0(\beta^3)$. 2.5.14

[where $0(\beta^3)$ indicates terms of the third order and greater

are neglected]. With no slippage the potential energy with respect to the equilibrium position, or position at rest, as datum (see Figure 2.10) is;

$$U = Mg(\bar{Y}-b)$$

By substituting for $\bar{Y}$ from equation 2.5.14,

$$U = Mg[b\{1+(\frac{a^2}{b^2} - 1/2)\beta^2\}-b]$$

$$= Mgb(\frac{a^2}{2b^2} - 1/2)\beta^2$$

For small oscillations, the kinetic energy according to Hannah and Stephen[9] is;

$$T = (1/2)I_b\dot{\beta}^2 + (1/2)Mb^2\dot{\beta}^2$$

Since harmonic oscillation is assumed;

$$\beta = \beta_o \sin\omega t.$$

Therefore, $U_{max.} = Mgb(\frac{a^2}{2b^2} - 1/2)\beta_o^2$,

$$T_{max.} = (1/2)I_b\beta_o^2\omega^2 + (1/2)MB^2\beta_o^2\omega^2$$

The moment of inertia about the minor axis is given by Carleton[5] as;

$$I_b = (1/5)M(a^2 + b^2).$$

Substituting for I_b gives,

$$T_{max.} = \frac{M}{10}(a^2 + 6b^2)\omega^2\beta_o^2$$

Recalling equation 2.2.3;

$$T_{max.} = U_{max.}$$

gives, $\frac{M}{10}(a^2 + 6b^2)\omega^2\beta_o^2 = Mgb(\frac{a^2}{2b^2} - 1/2)\beta_o^2$

Hence, $\omega^2 = \frac{5g(\frac{a^2}{b^2} - 1)}{b(\frac{a^2}{b^2} + 6)}$

$$f_n = \frac{1}{2\pi}\sqrt{\frac{5g(\frac{a^2}{b^2} - 1)}{b(\frac{a^2}{b^2} + 6)}} . \qquad 2.5.15$$

Equation 2.5.15 shows that the natural rocking frequency depends on the geometry of the prolate spheroid and not its mass.

The equation was used to calculate the natural rocking frequencies of the prolate spheroids in Table 2.1. The experimental and computed results are shown in Table 2.2.

TABLE 2.2

NATURAL ROCKING FREQUENCIES OF TWO PROLATE SPHEROIDS

Prolate Spheroids	a (in.)	b (ins.)	f_n(exp.)	f_n(comp.)
Steel	2.00	1.00	150	230
Aluminium	1.25	0.50	186	388

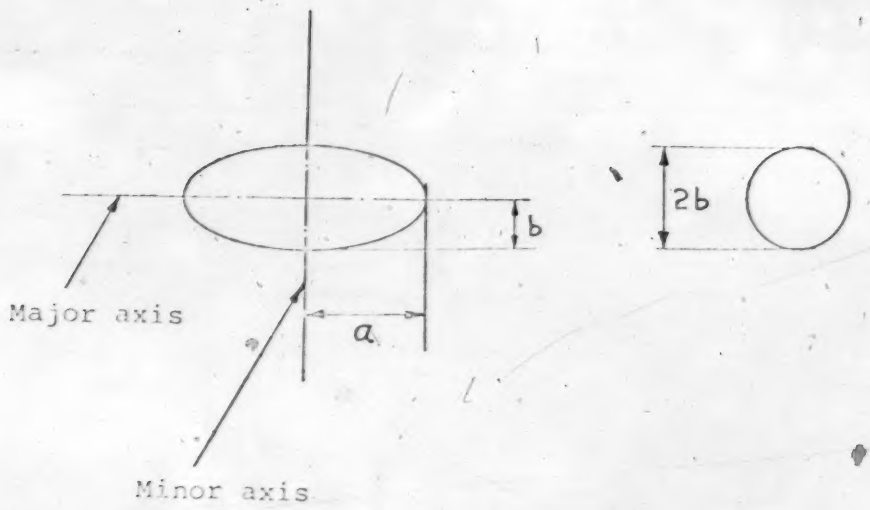

Figure 2.11 Schematic of Prolate Spheroid

2.4.3 Results, Discussion and Conclusions

Figures 2.12(a), 2.12(b), 2.13(a) and 2.13(b) show prints of parts of a movie film taken during the observation of prolate spheroid orientations on an oscillating pan. In Figure 2.12(a) the aluminium spheroid with a natural rocking frequency of 186 CPM (experimental) has an orientation with its major axis perpendicular to the direction of pan motion; the pan frequency being 150 CPM. In Figure 2.13(a), the orientation of the spheroid is with the major axis parallel to the direction of pan motion at pan frequencies of 303 and 405 CPM. Figure 2.12(b) shows the orientation of a wheat kernel with the major axis perpendicular to the direction of pan motion at pan frequencies of 303 and 405 CPM. In Figure 2.13(b), the orientation of the wheat kernel is with the major axis

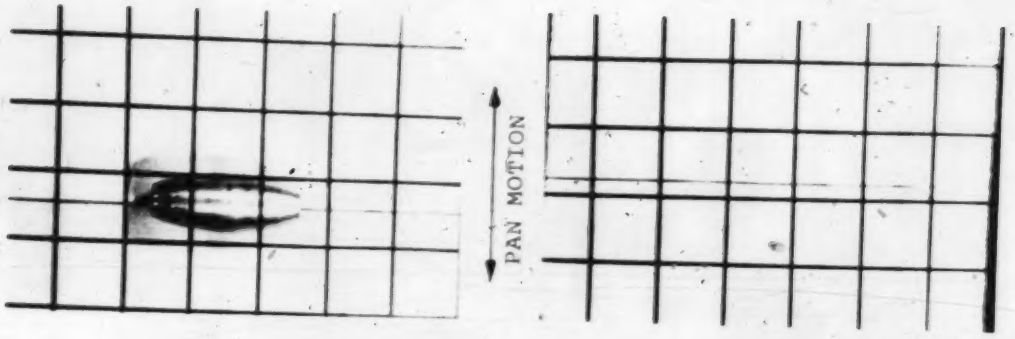

Figure 2.12(a)

Steel Prolate Spheroid
- Rolling Motion

Pan Frequency

Figure 2.12(b)

Wheat Kernel -
Rolling Motion

Natural Rocking Frequency

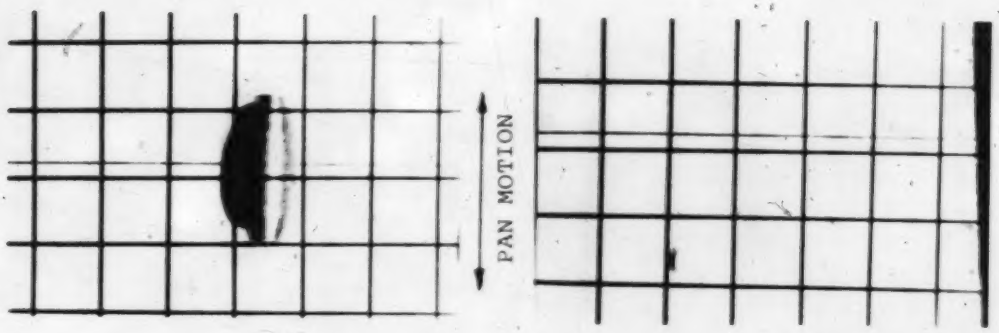

Figure 2.13(a)

Steel Prolate Spheroid
- Rocking Motion

Pan Frequency

Figure 2.13(b)

Wheat Kernel -
Rocking Motion

Natural Rocking Frequency

parallel to the direction of pan motion at pan frequencies of 500 and 620 CPM. Hence the natural rocking frequency of the kernel used is between 405 and 500 CPM. Using equation 2.5.15, the computed natural rocking frequency of the wheat kernel is 995 CPM which is nearly twice that indicated by its orientation on the oscillating pan. For the aluminium spheroid, the computed natural rocking frequency is more than twice the observed; and about 1 1/2 times for the steel spheroid (see Table 2.2).

Part or all of the differences between the computed and experimental natural rocking frequencies may be due to the objects not being perfect prolate spheroids. Thus, the usefulness of equation 2.5.15 is limited.

CHAPTER III

EQUATIONS OF KERNEL MOTION

3.1 Introduction

The motion of a kernel on an oscillating pan is the result of gravity and friction forces; the later a complex function of the coefficient of friction, the inertia of the kernel and the motion of the pan. As noted in the prior chapter, various modes of prolate spheroid motion ensued from changes in pan frequencies and slopes. Hence, it is evident that no one set of equations of motion can be applicable to all modes. Since each mode has a different set of forces acting on the kernel, equations of motion are derived separately for each mode by summing forces acting on the kernel in two planes; parallel and perpendicular to the pan surface. The notations used in deriving the equations are provided in Appendix A.

3.2 Assumptions

In deriving equations of motion for a kernel on an oscillating pan various assumptions have been made. They are as follows;

(1) It is assumed that there is no interference between the kernels and that the kernels do not contact the pan walls. With this assumption, the analysis can be restricted

to the response of a single kernel to the sinusoidal acceleration of the pan. Because the forces due to kernel interaction are not accounted for by this method, single kernels were used in determining the average experimental kernel velocity as will be seen later. For kernel interference, one must use appropriate laws of probability because the method used here is not appropriate.

(2) The pan is assumed to be flat and rigid. There was no visual evidence that the pan used to verify the results distorted when in operation.

(3) The kernel is assumed to be rigid and is not deformed by the forces experienced on the pan. Kernels are usually hard and rigid.

(4) The kernel is assumed to be a prolate spheroid.

(5) Rolling resistance is assumed to be negligible. Rolling resistance originates from the deformation of the kernel or the deformation of the surface on which the kernel is rolling[16] or both. Since both kernel and surface are assumed to be rigid and undeformable, the rolling resistance is neglected.

(6) The kinetic coefficient of friction between the kernel and pan surface is assumed constant and independent of slip velocity.

(7) The effect of air motion is neglected for the modes of motion in which the kernel is in contact with the pan.

(8) In the hopping mode, if the kernel does slides, the profile of the motion is as shown in Figure 3.1 but if not, the profile is as shown in Figure 3.2. However, sliding

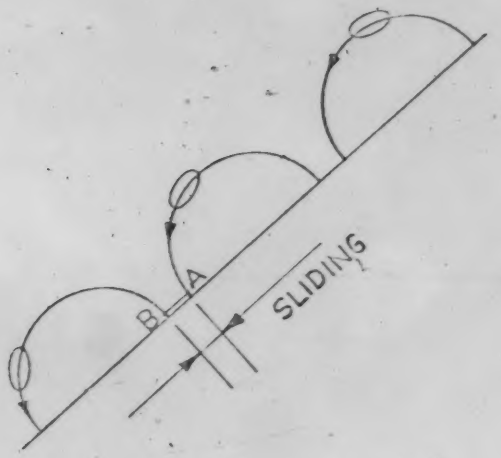

Figure 3.1 Hopping with sliding

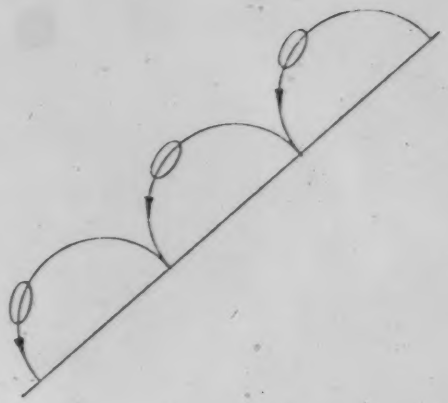

Figure 3.2 Hopping without sliding

was not detected. From observations the kernel leaves the pan at a pan frequency greater than 10 Hz. The contact period between the kernel and the pan must occur within one cycle and therefore must be less than one tenth of a second. This period is too short for any appreciable sliding to occur and therefore any sliding is neglected.

(9) The motion of the pan is assumed to be in the horizontal direction only. As shown in Figure 2.1(b), if the displacement h is small compared to R, the vertical displacement can be ignored. The vertical displacement of

B is Y;

where $Y = R(1-\cos\gamma)$

For the experimental pan, R is 12 in. and

$$h_{max.} \simeq r_{max.} = 0.75 \text{ in.},$$

therefore, $\sin\gamma = h/R = 0.75/12 = 0.062$.

Hence, $\gamma < 5°$

$$\cos\gamma \simeq 0.99 \simeq 1$$

and $Y = R(1-\cos\gamma) \simeq 0$

Hence, $\dot{Y}$, $\ddot{Y}$ are also negligible. This implies that the motion of G (see Figure 2.1(a)) is also horizontal since GC is rigid.

The effect of assumptions 1, 3 and 5 is that the only forces acting on the kernel are caused by the sinsusoidal acceleration of the pan and gravity when the kernel is in contact with the pan; having neglected forces due to rolling resistance, kernel interaction and pan wall effects.

3.3 Motion of Oscillating Pan

From the geometry of Figure 2.1(b);

$$A = L\sin\phi + r\sin\theta \qquad 3.4.1$$

$$S = L\cos\phi + r\cos\theta \qquad 3.4.2$$

From equation 3.4.1

$$L\sin\phi = A - r\sin\theta$$

$$\sin\phi = \frac{A - r\sin\theta}{L}$$

But $\cos\phi = \sqrt{1-\sin^2\phi}$

$$= \sqrt{1-\left(\frac{A-r\sin\theta}{L}\right)^2}$$

$$\simeq 1-\frac{(A-r\sin\theta)^2}{2L^2} + \frac{(A-r\sin\theta)^4}{8L^4} + \ldots. \qquad 3.4.3$$

$$\frac{(A-r\sin\theta)}{2L}_{max.} = 0.17$$

Hence, $\frac{(A-r\sin\theta)^4}{8L^4} = \frac{(1.55)^4}{8\times(4.5)^4} \ll 1$

Therefore equation 3.4.3 is approximately;

$$\cos\phi \simeq 1-\frac{(A-r\sin\theta)^2}{2L^2}$$

Substituting in 3.4.2

$$S = L\{1-\frac{(A-r\sin\theta)^2}{2L^2}\} + r\cos\theta$$

$$= L\{1-\frac{A^2}{2L^2} + \frac{2Ar\sin\theta}{2L^2} - \frac{r^2\sin^2\theta}{2L^2}\} + r\cos\theta$$

$$= L-\frac{A^2}{2L} + \frac{2Ar\sin\theta}{2L} - \frac{r^2\sin^2\theta}{2L} + r\cos\theta$$

$$\dot{S} = \dot{\theta}\{\frac{Ar\cos\theta}{L} - \frac{r^2\sin 2\theta}{2L} - r\sin\theta\}$$

$$\ddot{S} = \ddot{\theta}\{\frac{Ar\cos\theta}{L} - \frac{r^2\sin 2\theta}{2L} - r\sin\theta\}$$

$$+ \dot{\theta}^2\{-\frac{Ar\sin\theta}{L} - \frac{r^2\cos 2\theta}{L} - r\cos\theta\}$$

But $\ddot{\theta} = 0$ since ω = constant.

$\dot{\theta} = \omega$

Hence, $\ddot{S} = -\omega^2 r\{\frac{A\sin\theta}{L} + \frac{r\cos 2\theta}{L} + \cos\theta\}$ 3.4.4

For the oscillating pan used (see Figure 2.1):

$A_{max.} = 3.33$ in.,

$L = 4.5$ in.,

Therefore $\frac{r}{L} = \frac{r_{max}}{L} = \frac{0.75}{4.5} = 0.166.$

The maximum r used was 0.325 in.

Thus, $(r\cos 2\theta)/L$ is negligible.

Equation 3.4.4 is approximately;

$$\ddot{S} = -\omega^2 r(\frac{A\sin\theta}{L} + \cos\theta) \qquad 3.4.5$$

It can be seen that equation 3.4.5 describes simple harmonic motion. With a pan slope α (see Figure 3.4), the accelerations of the pan parallel and perpendicular to the pan surface are:

$$\ddot{X}_s = -\omega^2 r[\cos\theta + (\frac{A}{L})\sin\theta]\cos\alpha \qquad 3.4.6$$

$$\ddot{Y}_s = -\omega^2 r[\cos\theta + (\frac{A}{L})\sin\theta]\sin\alpha \qquad 3.4.7$$

3.4.1 Rolling and Sliding Mode

As noted previously in the rolling and sliding mode, two phases of kernel motion, rolling with sliding and rolling without sliding, can occur in a crank cycle. In these phases, four regimes of motion, normal roll down, reverse roll down, normal roll up and reverse roll up, can occur. The above

regimes, which are defined in detail in Table 3.1, are a result of the changing directions of the angular velocity and acceleration of the kernel motion on the oscillating pan. The positive senses of the various quantities are in the directions indicated by the arrows in Figure 3.3.

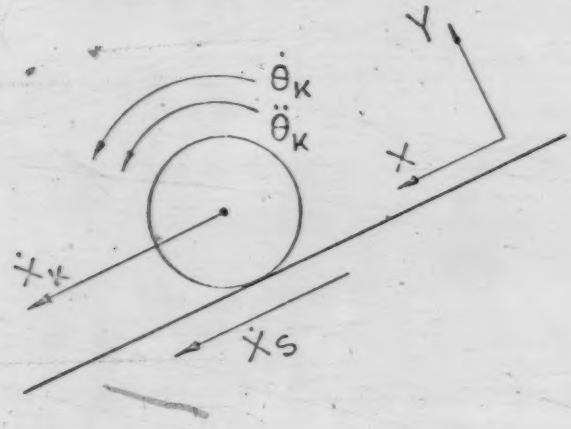

Figure 3.3 Velocities and accelerations of pan and kernel

TABLE 3.1

REGIMES OF KERNEL MOTION

	Normal Roll Down	Reverse Roll Down	Normal Roll Up	Reverse Roll Up
$\dot{\theta}_k$	>0	>0	<0	<0
$\ddot{\theta}_k$	>0	<0	<0	>0
$\dot{X}_s$	<0	<0	>0	>0
$\dot{X}_k$	>0	>0	<0	<0

3.4.2 Rolling With Sliding Phase

When a kernel is rolling and sliding simultaneously (rolling with sliding) on the pan surface;

$$\dot{X}_k > \dot{X}_s + b\dot{\theta}_k$$

The external and inertia forces acting on the kernel in the normal roll down regime with sliding are shown in Figure 3.4.

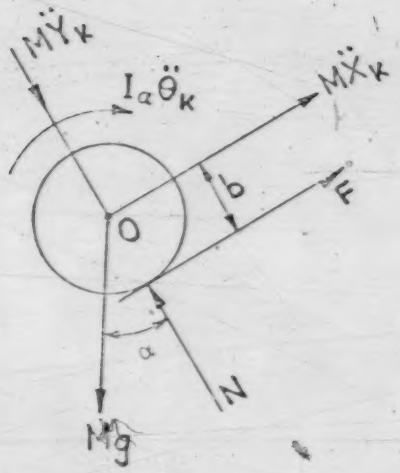

Figure 3.4 Free-body diagram of kernel in the normal roll down mode with sliding.

The equation for equilibrium of the force system in the direction parallel to the pan surface is;

$$Mg\sin\alpha - F = M\ddot{X}_k$$

$$F = Mg\sin\alpha - M\ddot{X}_k$$

$$= M(g\sin\alpha - \ddot{X}_k) \qquad 3.5.1$$

The equation for equilibrium of the force system in the direction perpendicular to the pan surface is;

$$N - Mg\cos\alpha = M\ddot{Y}_k$$

$$N = Mg\cos\alpha + M\ddot{Y}_k$$

$$= M(g\cos\alpha + \ddot{Y}_k) \qquad 3.5.2$$

The equation for equilibrium of the force system for rotation about the mass centre is;

$$Fb - I_a\ddot{\theta}_k = 0$$

$$F = (I_a\ddot{\theta}_k)/b.$$

According to Carleton[5] the mass moment of inertia about the major axis of a prolate spheroid is;

$$I_a = (2/5)Mb^2.$$

Hence, $F = (2/5)Mb\ddot{\theta}_k$ 3.5.3

Since the kernel slides as well as rolls, the friction force F is;

$$F = \mu_k N$$

Substituting for N from equation 3.5.2

$$F = \mu_k . M(g\cos\alpha + \ddot{Y}_k) \qquad 3.5.4$$

Equating equations 3.5.3 and 3.5.4:

$$(2/5)Mb\ddot{\theta}_k = \mu_k . M(g\cos\alpha + \ddot{Y}_k)$$

$$\ddot{\theta}_k = (5/2b)\mu_k[g\cos\alpha + \ddot{Y}_k] \qquad 3.5.5$$

Since the kernel is in contact with the pan, the acceleration of the pan perpendicular to the pan and the acceleration of the kernel are equal; that is,

$$\ddot{Y}_s = \ddot{Y}_k$$

Substituting $\ddot{Y}_s$ from equation 3.4.7 in equation 3.5.5;

$$\ddot{\theta}_k = (5/2b)\mu_k\{g\cos\alpha - \omega^2 r\sin\alpha[\cos\theta + (A/L)\sin\theta]\} \qquad 3.5.6$$

As the kernel is slipping, then equation 3.5.1 can be;

$$F = M(g\sin\alpha - \ddot{X}_k) = \mu_k N$$

Substituting for N from equation 3.5.2

$$M(g\sin\alpha - \ddot{X}_k) = \mu_k . M(g\cos\alpha + \ddot{Y}_k)$$

$$\ddot{X}_k = g\sin\alpha - \mu_k(g\cos\alpha + \ddot{Y}_k)$$

But $\ddot{Y}_k = \ddot{Y}_s$

Hence, $\ddot{X}_k = g\sin\alpha - \mu_k\{g\cos\alpha - \omega^2 r\sin\alpha[\cos\theta + (A/L)\sin\theta]\}$

3.5.7

Equations 3.5.6 and 3.5.7 are the equations for rotational and linear accelerations of a kernel in the normal roll down regime with sliding. The other regimes of this mode (reverse roll down etc.) are merely changes in the directions of the accelerations and therefore the equations apply to the other cases.

3.4.3 Rolling Without Sliding Phase

If the kernel rolls without sliding, then its velocity can be expressed as;

$$\dot{X}_k = \dot{X}_s + b\dot{\theta}_k \quad \text{from which,}$$

$$\ddot{X}_k = \ddot{X}_s + b\ddot{\theta}_k \qquad 3.5.8$$

Equating equations 3.5.1 and 3.5.3:

$$M(g\sin\alpha - \ddot{X}_k) = (2/5)Mb\ddot{\theta}_k$$

or $$g\sin\alpha - \ddot{X}_k = (2/5)b\ddot{\theta}_k \qquad 3.5.9$$

Substituting for $\ddot{X}_k$ from equation 3.5.8;

$$g\sin\alpha - \ddot{X}_s - b\ddot{\theta}_k = (2/5)b\ddot{\theta}_k$$

$$\ddot{\theta}_k = (5/7b)[g\sin\alpha - \ddot{X}_s]$$

Substituting for $\ddot{X}_s$ from equation 3.4.6;

$$\ddot{\theta}_k = (5/7b)\{g\sin\alpha + \omega^2 r\cos\alpha[\cos\theta + (A/L)\sin\theta]\} \qquad 3.5.10$$

From equation 3.5.8:

$$\ddot{\theta}_k = (1/b)(\ddot{X}_k - \ddot{X}_s) \qquad 3.5.11$$

From equation 3.5.9:

$$\ddot{X}_k = g\sin\alpha - (2/5)b\ddot{\theta}_k$$

Substituting for $\ddot{\theta}_k$ from equation 3.5.11:

$$\ddot{X}_k = g\sin\alpha - (2/5)b.(1/b)(\ddot{X}_k - \ddot{X}_s)$$

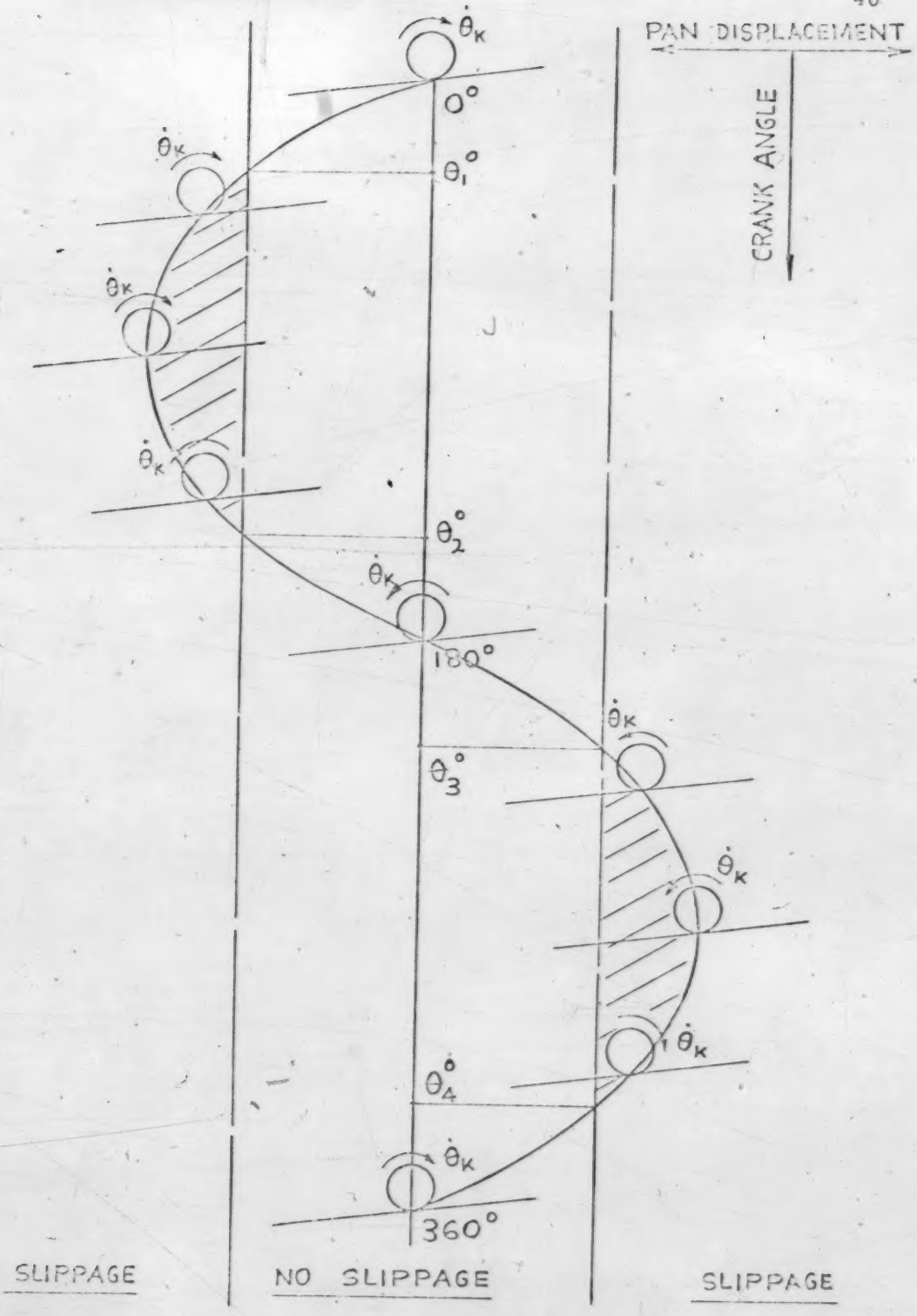

Figure 3.5 Rolling With and Without Sliding Motion.

$$\text{or} \quad (7/5)\ddot{X}_k = g\sin\alpha + (2/5)\ddot{X}_s$$

Substituting for $\ddot{X}_s$ from equation 3.4.6;

$$\ddot{X}_k = (5/7)\{g\sin\alpha - (2/5)\omega^2 r\cos\alpha[\cos\theta + (A/L)\sin\theta]\} \qquad 3.5.12$$

Equations 3.5.10 and 3.5.12 are the equations for rotational and linear accelerations of a kernel when it rolls without sliding.

Figure 3.5 shows the phases for rolling with sliding (slippage) and rolling without sliding. The equations for each phase would have to be applied separately if both occur in one crank cycle; that is, the equations for rolling without sliding would be applied from $0°$ to $\theta_1°$, $\theta_2°$ to $\theta_3°$ and $\theta_4°$ to $360°$ while the equations for rolling with sliding are applied from $\theta_1°$ to $\theta_2°$ and $\theta_3°$ to $\theta_4°$.

3.5 Rocking and Sliding Mode

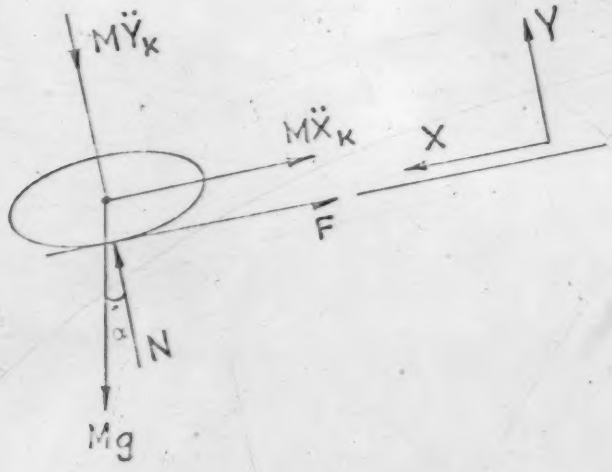

Figure 3.6 Free-body diagram of kernel sliding down the pan surface.

The equation of equilibrium of the force system in the direction parallel to the pan surface is;

$$Mg\sin\alpha - F = M\ddot{X}_k$$

$$\ddot{X}_k = -(F/M) + g\sin\alpha$$

But $F = \mu_k N$

Hence, $\ddot{X}_k = -(\mu_k N)/M + g\sin\alpha$ 3.6.1

The equation of equilibrium of the force system in the direction perpendicular to the pan surface is;

$$N - Mg\cos\alpha = M\ddot{Y}_k$$

$$N = M(\ddot{Y}_k + g\cos\alpha)$$

Substituting for N in 3.6.1:

$$\ddot{X}_k = -\mu_k(\ddot{Y}_k + g\cos\alpha) + g\sin\alpha$$

Substituting for $\ddot{Y}_k$ from equation 3.4.7:

$$\ddot{X}_k = \mu_k\{\omega^2 r\sin\alpha[\cos\theta + (A/L)\sin\theta] - g\cos\alpha\} + g\sin\alpha \quad 3.6.2$$

When the kernel is sliding up the pan surface, the equation of equilibrium of the force system in the direction parallel to the pan surface is;

$$F + Mg\sin\alpha = M\ddot{X}_k$$

$$\ddot{X}_k = (F/M) + g\sin\alpha$$

$$= (\mu_k N)/M + g\sin\alpha \quad 3.6.3$$

The equation of equilibrium of the force system in the direction perpendicular to the pan surface is;

$$N - M\ddot{Y}_k - Mg\cos\alpha = 0$$

$$N = M(g\cos\alpha + \ddot{Y}_k)$$

Substituting for N in equation 3.6.3;

$$\ddot{X}_k = \mu_k(g\cos\alpha + \ddot{Y}_k) + g\sin\alpha$$

Substituting for $\ddot{Y}_k$ from equation 3.4.7 ($Y_k = Y_s$);

$$\ddot{X}_k = \mu_k\{g\cos\alpha - \omega^2 r\sin\alpha[\cos\theta + (A/L)\sin\theta]\} + g\sin\alpha \qquad 3.6.4$$

Equations 3.6.2 and 3.6.4 are the equations of motion for a kernel sliding down and up respectively on the pan surface in the rocking and sliding mode.

3.6 Spinning and Sliding Mode

No attempt is made to derive equations of motion for the spinning and sliding mode because the torque producing the spinning effect on the kernel is not apparent. It is not known to what extent the torque affects the magnitudes of the forces acting on the kernel in the directions parallel and perpendicular to the pan surface.

3.7 Hopping Mode

The equations for the hopping mode have been derived elsewhere[10] since the kernel leaves the pan surface under the accelerations given by equations 3.6.2 and 3.4.7, therefore

the initial velocities of trajectory parallel and perpendicular to the pan surface must be obtained from the first integrals with respect to time of these equations.

CHAPTER IV

RESULTS, DISCUSSION, SUMMARY AND CONCLUSIONS.

4.1 Experimental Kernel Velocities.

The average velocities of a wheat kernel on the oscillating pan for the rocking and sliding mode were determined by timing the kernel to travel over a distance of 18.0 in. on the pan surface. Figure 4.1 shows the pan surface ABCD with two lines GH and EF 18.0 in. apart.

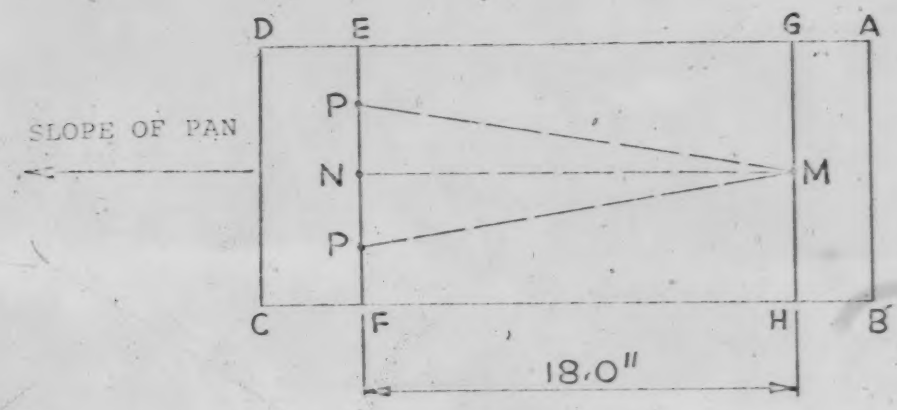

Figure 4.1 Kernel Path on Pan Surface.

For each combination of pan frequency, slope and crank radius, three successful runs were made. If the kernel followed a path between MN and MP, the run was recorded, otherwise it was rejected; where the angle PMN was less than five degrees. The number of rejected runs did not exceed three. Table 4.1 shows the average velocities for the three successful runs at

TABLE 4.1

EXPERIMENTAL WHEAT KERNEL VELOCITIES.

Frequency (Rads/sec.)	Crank Radius (In.)	Pan Slope (Rads)	$\dot{X}_{K(1)}$ (In./sec.)	$\dot{X}_{K(2)}$ (In./sec.)	$\dot{X}_{K(3)}$ (In./sec.)	Average Vel. (In./sec.)
54.2	0.15	0.037	1.75	1.65	1.85	1.75
54.2	0.20	0.037	2.30	2.15	2.15	2.20
54.2	0.28	0.037	2.50	2.60	2.40	2.50
54.2	0.33	0.037	2.80	2.65	2.80	2.75
64.9	0.20	0.078	5.05	5.10	4.85	5.00
64.9	0.20	0.110	5.85	5.65	5.75	5.75
64.9	0.20	0.145	7.15	6.95	7.26	7.12
64.9	0.20	0.179	8.66	8.78	8.15	8.53
54.2	0.20	0.078	4.30	4.10	4.35	4.25
54.2	0.20	0.110	4.85	4.75	4.95	4.85
54.2	0.20	0.145	6.05	6.30	6.10	6.15
54.2	0.20	0.179	7.26	7.08	7.35	7.23

various combinations of pan frequency, slope and crank radius.

4.2 Discussion of Results.

It is apparent that for prolate spheroid shaped seeds, the appropriate orientations of the screen aperatures depend on whether the screen is operated at frequencies below or above the natural rocking frequency of the seeds being graded.

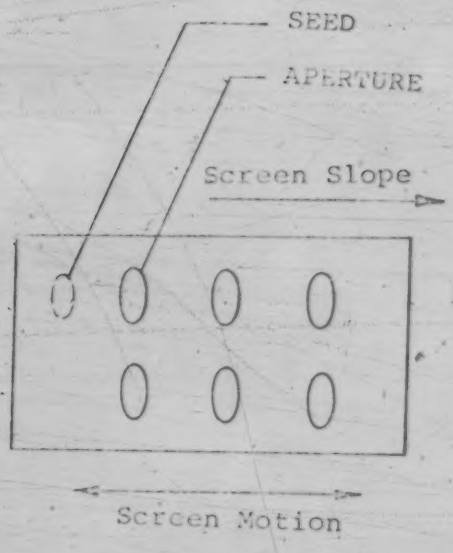

Figure 4.2 Aperture orientation for rolling and sliding seeds.

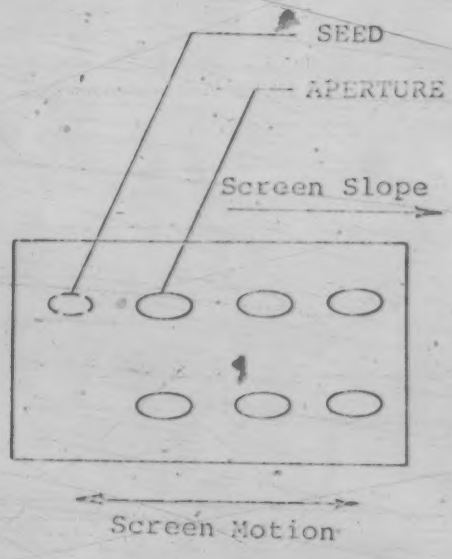

Figure 4.3 Aperture orientation for rocking and sliding seeds.

As shown in Figure 4.2, (for prolate spheroid shaped seeds) the screen should be operated at a frequency below the natural rocking frequency of the seeds in order to allow the undersized seeds to go through the apertures; whereas in Figure 4.3, the screen would have to be operated above the natural rocking frequency of the prolate spheroid shaped seeds to

allow the undersized seeds to go through the apertures.

The results in Table 4.1 show that the wheat kernel velocities increase with increase in each of the independent variables pan frequency, slope and crank radius; these being the variables of equations 3.6.2 and 3.6.4.

An observation of some seed cleaning operations showed that various frequencies, crank radii and screen slopes are used by different manufacturers. One manufacturer uses a minimum and maximum frequency of 150 and 635 CPM respectively, with an average frequency of 435 CPM. The crank radius of oscillation is 0.25 in. and the minimum and maximum screen slopes are 12.0° and 15.0° respectively, with no pitman inclination. Another manufacturer uses a minimum and maximum frequency of 150 and 485 CPM, with an average frequency of 450 CPM. The crank radius being 0.30 in. with a minimum and maximum screen slope of 16° and 20° respectively but no pitman inclination. Within the ranges specified, seed cleaners use various combinations of frequency, crank radius and screen slope depending on the type of seeds being cleaned and the amount of dirt to be removed.

Relating these observations to the analysis, it is apparent that the screens are operated in the first three modes of motion - rolling and sliding, rocking and sliding, spinning and sliding. These modes are only applicable to prolate spheroid shaped seeds such as wheat, oats, rye, barley, etc. The motion of non-prolate spheroid seeds such as flax

would be riding and sliding. Although the maximum frequency for one of the cleaners is as high as 635 CPM, there would be negligible hopping at this frequency with a low screen slope of 15°. As already noted, this mode is significantly influenced by both screen frequency and slope. Also sieving efficiency would be reduced in the hopping mode since the hopping effect would reduce the chances of the undersized seeds going through the apertures of the screen.

4.3 Summary and Conclusions.

The motion of a wheat kernel on an oscillating pan was studied. There are four modes of motion of the kernel, two of which are dependent on the natural rocking frequency of the wheat kernel and the frequency of oscillation of the pan. The four modes are, rolling and sliding, rocking and sliding, spinning and sliding and hopping. It was observed that the kernel orientation was with the major axis perpendicular to the direction of pan motion when the pan was operated at frequencies below the natural rocking frequency of the kernel. At pan frequencies above the natural rocking frequency of the kernel, the kernel orientation was with the major axis parallel to the direction of pan motion.

An expression was derived for the natural rocking frequency of a prolate spheroid. Using this expression, the natural rocking frequencies of various sizes of prolate spheroids were determined and their orientations on an

oscillating pan observed at various pan frequencies.

Equations of motion for kernel acceleration on the pan were derived for various modes of motion. The experimental velocities for the rocking and sliding mode increase in accordance with the derived equations.

BIBLIOGRAPHY

BIBLIOGRAPHY

1. Berry, P. E. 1958. Research on oscillating conveyors. Journal of Agricultural Engineering Research, 3(3).

2. Berry, P. E. 1959. Basic theory of low-acceleration oscillating conveyors. Journal of Agricultural Engineering, Research, 4(3).

3. Bottcher, S. 1958. Contribution to the problem of conveying materials by oscillating conveyors (Parts 1-111) (Translation No. 72, National Institute of Agricultural Engineering Silsoe, Britain). Fördern und Heben (3) 127-131; (4) 235-240; (5) 307-315.

4. Canada Committee on Agricultural Engineering, Canada Dept. of Agriculture. 1971. Agricultural material handling manual Part 2, Section 2.2:34-35.

5. Carleton, G. F. 1970. Engineering mechanics: statics and dynamics. Merrill Co. Ohio. United States.

6. Garvie, D. W. 1966. Operating conditions for maximum efficiency in the use of cleaning and grading machines for grain. Journal and Proceedings of the Institute of Agricultural Engineers, Britain, 22(4).

7. Goursat, H. 1904. Course in mathematical analysis Vol. 1. Ginn & Company, Cambridge.

8. Hann, S. D. and J. P. Gentry. 1970. Analysis and simulation of the motion of an ellipsoidal object on an oscillating conveyor. Paper No. 70-887, ASAE, St. Joseph, Michigan.

9. Hannah, J. and R. C. Stephen. 1970. Mechanics of machines (Elementary theory and examples). Edward Arnold Ltd., London, Britain.

10. Harrison, H. P. 1969. Kernel rebound trajectories in a combine shoe using analogue simulation. CAE 11(2).

11. Harrison, H. P. 1975. Simulated particle dynamics with combine walker. CAE 17(1).

12. Henderson, J. M. and A. M. Newman. 1972. Orientation of a prolate spheroid object. Trans. ASAE 15(6): 1128-1131.

13. Levi, H. 1960. Foundations of geometry and trigonometry. Prentice-Hall, Inc., New Jersey.

14. Schertz, C. E. and T. E. Hazen. 1963. Predicting motion of granular material on an oscillating conveyor. Trans. ASAE 6(1): 6-10.

15. Schertz, C. E. and T. E. Hazen. 1965. Movement of shelled corn on an oscillating conveyor. Trans. ASAE 8(4): 582-583.

16. Seely, F. B. and N. E. Ensign. 1921. Analytical mechanics for engineers. John Wiley & Sons, New York.

17. Shames, I. H. 1965. Mechanics of fluids. McGraw-Hill Book Co., Inc., New York.

18. Stein, S. K. 1971. Calculus. McGraw-Hill Book Company, New York, United States.

19. Thomson, W. T. 1971. Vibration theory and application. George Allen & Unwin Ltd., London, Britain.

APPENDIX A

BASIC NOTATION

The notation adopted in the derivation of the equations of motion are as follows:

$\dot{X}_K$, $\ddot{X}_K$ = kernel velocity and acceleration relative and parallel to the pan surface.

$\dot{Y}_K$, $\ddot{Y}_K$ = kernel velocity and acceleration relative and perpendicular to the pan surface.

$\dot{X}_S$, $\ddot{X}_S$ = pan velocity and acceleration perpendicular to the pan surface and relative to the ground.

$\dot{Y}_S$, $\ddot{Y}_S$ = pan velocity and acceleration perpendicular to the pan surface and relative to the ground.

r = crank radius.

I_a = mass moment of inertia of kernel about its major axis.

I_b = mass moment of inertia of kernel about its minor axis.

M = mass of kernel.

μ_s, μ_k = static and kinetic coefficients of friction between the kernel and pan surface.

$\dot{\theta}_k, \ddot{\theta}_k$ = angular velocity and acceleration of kernel relative to the pan surface.

f_n = natural rocking frequency of kernel.

ωt = crank angular displacement of pan's slider crank mechanism.

ω = pan frequency.

t = time.

α = pan slope.

APPENDIX B

DETERMINATION OF DIFFERENTIAL EQUATION CONSTANTS

The equation constants for the rocking and sliding mode were determined using the following procedures:

(1) The coefficients of friction μ_s and μ_K; the coefficients of friction between the wheat kernels and the pan surface were determined using an inclined plane AB (24 inches long) as shown in Figure A2.1.

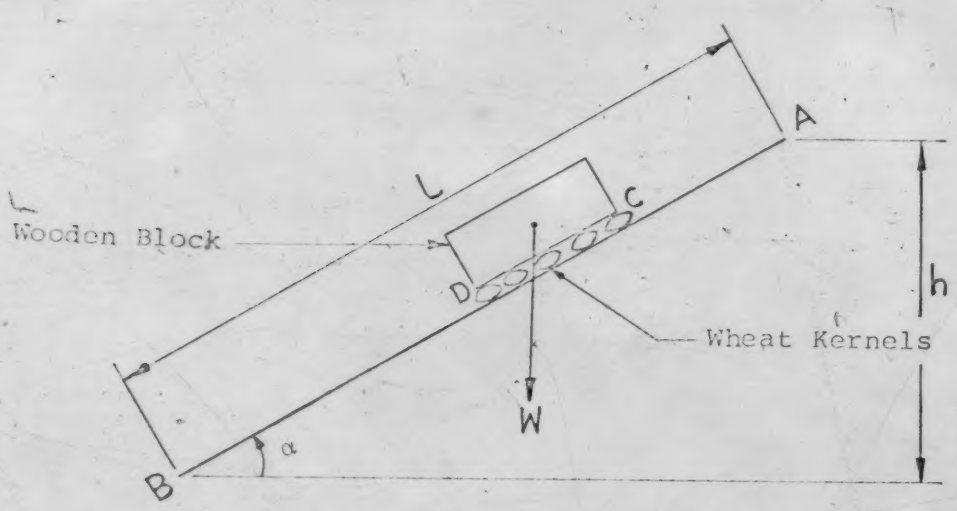

Figure A2.1 Inclined plane

The plane AB was covered with paper of the same surface roughness as used on the pan surface in determining the experimental average kernel velocities. Wheat kernels were glued to the surface CD of the wooden block so that the only contact between the block and the plane was through the wheat

kernels. The height h was increased by increasing the slope α until the block was about to slide down the plane. At this position the height, h_1, was recorded. Then the height was further increased until the block started to slide down the plane. To obtain steady state sliding, the height was lowered until the block was beginning to decelerate, then the height, h_2, was recorded. The whole experiment was repeated three times and the average values for h_1 and h_2 were calculated and recorded as shown;

h_1(average) = 8.20 in. (for static coefficient of friction)

h_2(average) = 7.70 in. (for kinetic coefficient of friction)

According to Carleton,[5] the static coefficient of friction is given by:

$$\mu_s = \tan\alpha_1$$

$$\alpha_1 = \sin^{-1}(h_1/AB)$$

$$= \sin^{-1}(8.20/24)$$

$$= 20°$$

Hence, $\mu_s = \tan 20$

$$= 0.3642$$

$$= 0.36$$

Similarly;

$$\mu_k = \tan\alpha_2$$

$$\alpha_2 = \sin^{-1}(7.70/24)$$

$$= 18.65°$$

Therefore, $\mu_k = \tan 18.65$

$$= 0.338$$

(2) Oscillating Frequency:

The oscillating frequencies of the pan were determined using the stroboscope. The unit of frequency used in the simulation is radians/sec.

(3) Crank Radius:

The crank radius was determined by measuring the length of a line drawn by a pencil fixed to the pan frame. The length of this line was divided by two to obtain the crank radius in inches which is the unit used in the simulation.

(4) Pan Slope:

The pan slope was determined by measuring the height of the ends of the pan above the horizontal and applying the known length of the pan. All angular measurements in the simulation were in radians.

(5) The standard value of acceleration under gravity 386.4 in./sec.^{2} was used.

(6) Pitman Inclination:

Using the appropriate values of pan slope and crank radius, β_1 was calculated from Figure 2.1. The pitman inclination β is the sum of β_1 and β_o.

(7) Constants - A and L

From Figure 2.1;

$A_1 = AB\sin\alpha$

$= 9\sin\alpha$

$A_o = 1.05$ in (Difference in elevation between B and O)

Hence, $A = 9\sin\alpha + 1.05$

$L = 4.5$ in.

The values of pitman inclination, (β), and the constant, A, are tabulated below for the combinations of pan frequency, slope and crank radius used in the simulation.

SIMULATION PARAMETERS

Crank Radius (In.)	Frequency (Rads)	Pan Slope (Rads)	Pitman Incl. (Rads)	A (In.)
0.15	54.2	0.037	0.310	1.4
0.20	54.2	0.037	0.306	1.4
0.28	54.2	0.037	0.302	1.4
0.33	54.2	0.037	0.300	1.4
0.20	64.9	0.078	0.392	1.75
0.20	64.9	0.110	0.466	2.04
0.20	64.9	0.145	0.550	2.35
0.20	64.9	0.179	0.645	2.65
0.20	54.2	0.078	0.392	1.75
0.20	54.2	0.110	0.466	2.04
0.20	54.2	0.145	0.550	2.35
0.20	54.2	0.179	0.645	2.65